JOURNAL OF CATALYSIS 129, 168–176 (1991)

Interaction of Arsenious Oxide with $DeNO_x$-Catalysts: An X-Ray Absorption and Diffuse Reflectance Infrared Spectroscopy Study

FRANK HILBRIG,*‡ HERBERT E. GÖBEL,† HELMUT KNÖZINGER,* HELMUT SCHMELZ,‡ AND BRUNO LENGELER§

*Institut für Physikalische Chemie, Universität München, Sophienstrasse 11, 8000 München 2, Germany; †Siemens Research Laboratories, München, Otto-Hahn-Ring 6, 8000 München 90, Germany; ‡Siemens AG, Power Generation Group KWU, Otto-Hahn-Ring 6, 8000 München 90, Germany; and §Institut für Festkörperforschung, Forschungszentrum Jülich, Postfach 1913, 5170 Jülich 1, Germany

Received August 6, 1990; revised November 30, 1990

The interaction of arsenious oxide with $deNO_x$-catalysts such as titania-supported oxides of molybdenum and tungsten has been studied by X-ray absorption spectroscopy (XANES and EXAFS) and by diffuse reflectance FT infrared spectroscopy (DRIFT). It is shown by XANES at the As K edge that the majority oxidation state of the arsenic surface species is As^{5+}. EXAFS beyond the As K edge indicates a (3 + 1) oxygen coordination shell around the arsenic with As–O distances of 1.67 and 1.94 Å, respectively. A characteristic new infrared hydroxyl stretching band at 3610 cm^{-1} is formed and can be assigned as an AsO–H stretching mode. These experimental results can best be associated with an orthoarsenate(V) surface species which forms when arsenious oxide is deposited on the catalyst surfaces. XANES at the W L_1 and W L_3 edges suggest that the orthoarsenate interacts directly with tungsten sites, a condition which is supported by the strong perturbation of the new W=O stretching overtone on formation of the arsenate. It is tentatively suggested that the poisoning of titania-supported tungsten oxide $deNO_x$-catalysts is due to blocking of active sites which involve coordinatively unsaturated tungsten centers by the orthoarsenate surface species.

INTRODUCTION

Besides combustion process modifications, the selective catalytic reduction (SCR) of NO with ammonia as the reducing agent (*1*) is the most successful method to diminish the nitrogen oxide emission in the tail gas from coal power plants. Commonly applied catalysts are mixed oxides of vanadium and molybdenum or tungsten supported on titania. The most potent poison for $deNO_x$-catalysts is diarsenic trioxide As_2O_3, which when deposited on the catalyst surface limits the lifetime of the catalysts (*2*). This is particularly severe in power plants with wet bottom boilers and ash recirculation where the arsenious oxide concentration in the tail gas is high (*3*). Although improvements on the resistance of $deNO_x$-catalysts toward arsenious oxide have been achieved by empirical means, the detailed mechanism of the arsenic poisoning is still unknown.

The present contribution aims at elucidating the modes of interaction of arsenious oxide with the surfaces of titania and titania-supported $deNO_x$-catalysts; the final goal of this study is to understand the details of the poisoning mechanism of arsenious oxide.

We used X-ray absorption spectroscopy (XAS) and infrared spectroscopy (IRS) to determine the valence state and the local environment around the arsenic and the interaction of the amorphous oxide of arsenic with the catalyst surface. The samples investigated in this study were laboratory specimens and a catalyst drawn from a pilot power plant after several thousand hours of operation.

EXPERIMENTAL

Catalyst Preparation and Poisoning Procedures

TiO_2–P25 and WO_3 were Degussa products with surface areas (BET, N_2) of 50 m^2/g

0021-9517/91 $3.00

and 43 m^2/g, respectively. The N_2-BET surface area of MoO_3, a Merck product, is unknown but is certainly below 5 m^2/g (*4*). Physical mixtures of 3 wt% WO_3/TiO_2, 9 wt% WO_3/TiO_2, 1.2 wt% MoO_3/TiO_2, and 4.1 wt% MoO_3/TiO_2 were ground in an agate mortar. Each mixture was separately calcined at 723 K in a moist oxygen stream (50 ml/min; $P(H_2O)$ = 18 mbar). For the WO_3/TiO_2 samples the calcination time was 12 h (samples TiW3A and TiW9A), and for the MoO_3/TiO_2 samples 30 h (samples TiMo1.2A and TiMo4.1A).

By X-ray diffraction and laser-raman spectroscopy it was confirmed that the spreading of WO_3 (*5*) and MoO_3 (*4*), respectively, was complete and that a highly dispersed phase of the supported oxide had formed. For TiO_2–P25 the monolayer capacity of supported tungsten oxide is reached at 9.3 wt% WO_3 (*6*) and of supported molybdenum oxide at 4.1 wt% MoO_3 (*7*). In this context the monolayer capacity is defined by the possible amounts of WO_3 and MoO_3, respectively, which can spread over the titania surface to a highly dispersed species.

Arsenious oxide was brought onto the samples by sublimation of As_2O_3 (Merck) at 673 K in an autoclave in air. The arsenious oxide content for these samples TiW3A(As), TiW9A(As), TiMo1.2A(As), and TiMo4.1A(As) was 2.5–3.5 wt%, as determined by the weight increase. An additional sample was prepared by grinding a physical mixture of 3 wt% As_2O_3 (Merck)/TiO_2–P25. A technical catalyst W188a with a Ti : Mo : V composition (at.%) of 92 : 6 : 2 was loaded with arsenious oxide by sublimation as described above (sample W188a(As)). Specimen H500p4400h was a piece of a catalyst metal plate with a Ti : Mo : V composition comparable to that of the catalyst W188a. This catalyst had operated in a pilot coal power plant for 4400 h.

X-Ray Absorption Spectroscopy

When X rays pass through matter, their intensity is attenuated. The relationship between the intensities $I_1(E)$ and $I_2(E)$ before and after passing through a layer of thickness d is

$$I_2 = I_1 \exp[-\mu(E)\, d].$$

The linear absorption coefficient $\mu(E)$ depends on the photon energy E and on the absorbing material. $\mu(E)$ shows edges at certain energies (E_0), which are characteristic for the absorber. Furthermore oscillations in μ are observed above an absorption edge if the system is not too strongly disturbed. This EXAFS (extended X-ray absorption fine structure) contains information on the geometric structure, i.e., the coordination numbers and the interatomic distances (*8–12*). At an As K edge arsenic 1*s* electrons are excited into empty 4*p* states.

The X-ray absorption experiments at the As K, W L_1, and W L_3 edges were carried out at the beam line E2 of the electron storage ring DORIS II (3.7 GeV, 40–100 mA) at HASYLAB (DESY Hamburg) using the experimental set-up described in Refs. (*13, 14*). The measurements were carried out in an *in situ* cell, which was designed for measurements in the transmission and fluorescence modes between 300 and 750 K in a defined gas atmosphere. For the XANES (X-ray absorption near-edge structure) experiments in the transmission mode at 77 K in N_2 and at 673 K in O_2 (20 ml/min), the sample powders TiW3A(As), TiW9A(As), TiMo1.2A(As), and TiMo4.1A(As) were lightly pressed into an aluminum frame (0.5 mm thick) over an area of 10 × 25 mm^2 and enveloped in aluminum foil. The ground physical As_2O_3/TiO_2 mixture and the arsenious oxide poisoned catalyst W188a(As) were pressed onto an expanded steel plate. Their As K XANES were measured at 300 K in air in the fluorescence mode. The reference compounds used for the As K XANES and EXAFS analysis were metallic arsenic (Koch–Light), As_2O_3 (Merck), As_2O_5 (Alfa), Ag_3AsO_4, and $KAsF_6$. The As K, W L_1, and W L_3 XANES spectra were normalized by fitting linear functions to the pre-edge data and to the data of the EXAFS

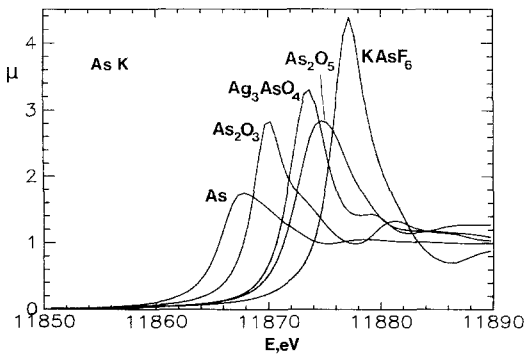

FIG. 1. Normalized As K XANES spectra of metallic As, As_2O_3, Ag_3AsO_4, As_2O_5, and $KAsF_6$.

region, extrapolating both functions to the zero of energy E_0, subtracting the pre-edge data function from every point in the experimental spectrum and dividing by the step height at E_0. This results in normalizing the data to unit step height. The oscillatory part of the absorption beyond the As K edge (EXAFS) was extracted from the total absorption and normalized to the jump height according to the procedure described in Ref. (*9*). Then the abscissa of the normalized EXAFS (E) was converted from the photon energy E to the wavenumber k. The data (k = 2–13 $Å^{-1}$) were weighted by k^2 and Fourier transformed (*8–10*).

Diffuse Reflectance Infrared Spectroscopy

The DRIFT (diffuse reflectance infrared Fourier transform) spectra were measured *in situ* at 673 K in flowing O_2 (100 ml/min) with a Bruker IFS 88 spectrometer equipped with an *in situ* cell (Spectratech). The spectral resolution was 5 cm^{-1}.

RESULTS AND DISCUSSION

XANES at As K edge

Figure 1 shows the linear absorption coefficient for the reference compounds metallic arsenic, As_2O_3, Ag_3AsO_4, As_2O_5, and $KAsF_6$ in the vicinity of the As K edge. The position of the edge is shifted to higher energy with increasing valence of arsenic due to a higher effective nuclear charge and a reduced electron screening. Arsenic in Ag_3AsO_4 is tetrahedrally surrounded by oxygen (*15*), whereas As_2O_5 is composed of equal numbers of AsO_4 tetrahedra and AsO_6 octahedra, the latter having longer As–O distances (*16*). The energy shifts ΔE (eV) of the K edge of the various reference compounds relative to the position of the As K edge of metallic arsenic are listed in Table 1. The energy difference between trivalent arsenic in As_2O_3 and pentavalent arsenic in Ag_3AsO_4 and As_2O_5 is +3.7 and +4.8 eV, respectively. This indicates that besides the formal charge the coordination number and As–O bond distances also have an effect on the edge position (*14*). However, as can be seen in Fig. 1, the oxidation state of the arsenic is the dominant factor as long as the ligands are exclusively oxygens. Only when highly electronegative ligands such as fluorine are involved, as in $KAsF_6$ (see Fig. 1 and Table 1), is an additional shift of the As K edge position to still higher energy observed. Therefore, these characteristics can be used as a "fingerprint" to determine the valence of arsenic in the arsenic oxide poisoned samples.

It should be mentioned that the chemical shift of +2.5 eV observed in the present study for trivalent arsenic in As_2O_3 differs significantly from the values reported by Agarwal and Verma (*17*) and by Sapre and Mande (*18*) who measured +4.5 eV and +6.3 eV, respectively, with conventional X-ray tubes.

Based on the data of Fig. 1 and Table 1, the features of the normalized As K absorption edges of samples TiW3A(As) (Fig. 2a) and TiW9A(As) (Fig. 2b), measured at

TABLE 1

Energy Shift ΔE(eV) of the As K Edge of Various Arsenic Compounds Relative to Metallic As

	ΔE [eV]
As_2O_3	+2.5
Ag_3AsO_4	+6.2
As_2O_5	+7.3
$KAsF_6$	+9.6

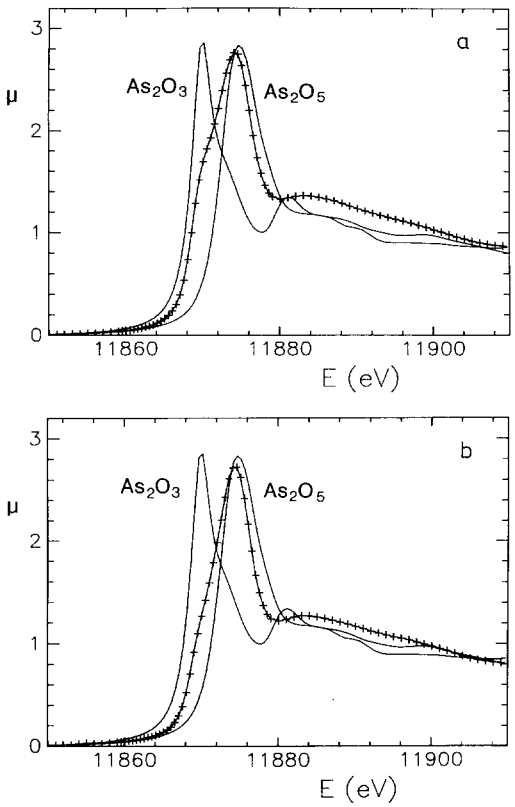

FIG. 2. (a) Normalized As K XANES spectrum of TiW3A(As) at 673 K in O_2 (+). The spectra of As_2O_3 and As_2O_5 are included for comparison. (b) Normalized As K XANES spectrum of TiW9A(As) at 673 K in O_2 (+). The spectra of As_2O_3 and As_2O_5 are included for comparison.

673 K in O_2, in comparison with those of As_2O_3 and As_2O_5, demonstrate that the arsenic atoms are mainly pentavalent. Only the sample TiW3A(As), i.e., the sample with $\frac{1}{3}$ monolayer of tungsten oxide on titania, has a significant portion of As^{3+}. This can be seen by the shoulder on the low-energy side of the absorption edge (Fig. 2a). In contrast, comparably small relative amounts of As^{3+} are present on the monolayer WO_3/TiO_2 sample, TiW9A(As). Entirely analogous results were obtained for arsenic oxide covering the two MoO_3/TiO_2 samples TiMo1.2A(As) and TiMo4.1A(As) with low and high molybdenum oxide loading, respectively. Even when TiO_2–P25 and As_2O_3(Merck) were simply ground in an agate mortar, the trivalent arsenic was oxidized to a significant extent (Fig. 3). Moreover, the sample W188a(As) and the specimen H500p4400h drawn from the power plant, each with comparable Mo/V/Ti composition, contained exclusively pentavalent arsenic. The chemical shift values ΔE for As^{5+} were constant at +6.7 eV for all investigated samples, and thus fall exactly between the chemical shifts of As^{5+} in Ag_3AsO_4 (+6.2 eV) and of As^{5+} in As_2O_5 (+7.3 eV). This fact already indicates that the pentavalent surface oxide can neither be described as a pure arsenate nor as an amorphous arsenic pentoxide As_2O_5.

It is worth mentioning that the formation of As^{5+} on evaporation of As_2O_3 onto pure titania has also been confirmed by XPS (*19a*), while Rademacher *et al.* (*19b*) detected both As^{3+} and As^{5+} on a technical catalyst H500p similar to the one studied in this work. This discrepancy may well be due to somewhat different operation conditions for the two specimens.

EXAFS beyond the As K edge

In addition to the positions of the As K edges of all samples their EXAFS modulations are also identical. These observations indicate that a deposition of arsenious oxide by sublimation onto the catalyst surface

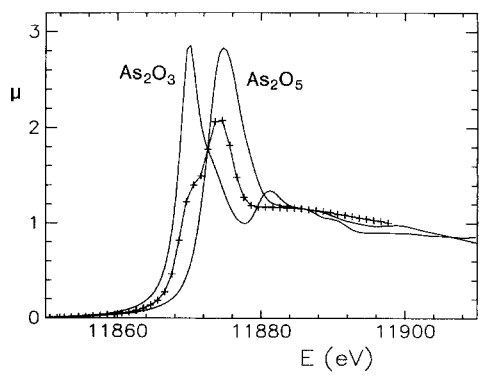

FIG. 3. Normalized As K XANES spectrum of a physical As_2O_3/TiO_2 mixture at 300 K in air (+). The spectra of As_2O_3 and As_2O_5 are included for comparison.

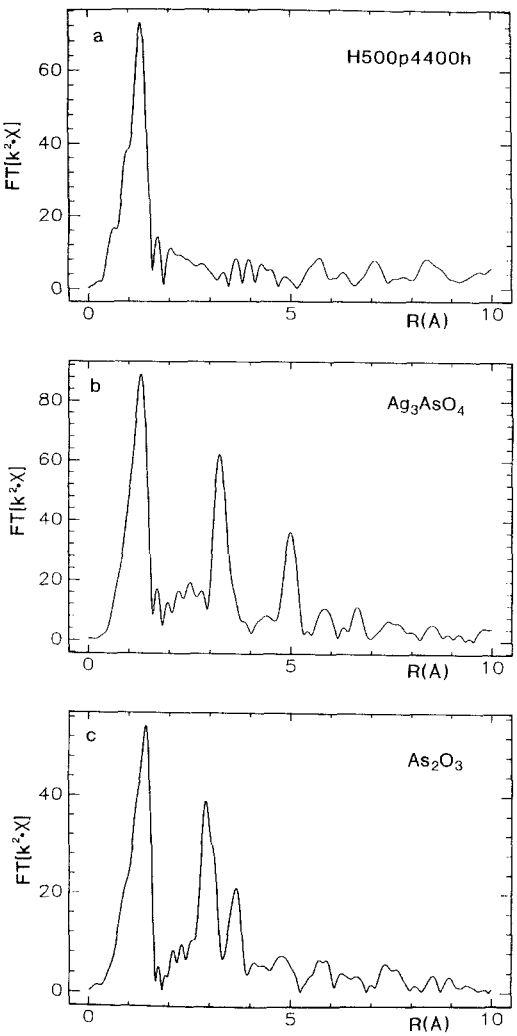

FIG. 4. Fourier transform of the EXAFS $k^2\chi$ beyond the As K edge of H500p4400h (a), Ag_3AsO_4 (b), and As_2O_3 (c).

at elevated temperature, e.g., sample W188a(As), and poisoning by operation of a catalyst in a coal power plant for an extended period (specimen H500p4400h) lead to identical surface species. Because in H500p4400h all arsenic atoms were found to be pentavalent, the EXAFS of this sample, measured at 77 K in N_2, was used as an example for all other samples to analyze the geometric structure around the As^{5+} atoms. Figure 4a displays the Fourier transformed EXAFS $k^2\chi$ of H500p4400h. This spectrum shows that the As^{5+} has only short-range order of oxygen atoms. Figures 4b and 4c are the EXAFS spectra of Ag_3AsO_4 and As_2O_3. The corrected As^{5+}–O distances r_j and oxygen coordination numbers N_j were calculated for H500p4400h by a nonlinear curve-fitting analysis (*10*). The peak in the noncorrected EXAFS spectrum of H500p4400h (R=0.5–1.9 Å) was isolated with a window and Fourier backtransformed. The first oxygen shells in Ag_3AsO_4 (R=0.5–1.9 Å) and in As_2O_3 (R=0.5–1.9 Å) were treated in the same way. From the former the As–O phase shift and backscattering functions including the inelastic loss factor were extracted. In cubic Ag_3AsO_4 (*15*) the arsenic is ideally surrounded tetrahedrally by oxygen. Its As–O distance, however, is not as yet precisely established. However, according to recent structure analyses of 10 different arsenate compounds, (*15*), the As–O distance in arsenates is rather independent of the cations in the compounds and equal to 1.68(±0.01) Å. The zero of energy was the first point of inflection in the As K edge of Ag_3AsO_4. With these data and the As–O phase shift and backscattering functions, curve fits on the isolated EXAFS from the first oxygen shell around arsenic in H500p4400h and in As_2O_3 were carried out. The results of these analyses are given in Table 2. Figure 5 shows the quality of the curve fit for H500p4400h. In cubic As_2O_3 (arsenolith) the arsenic is coordinated in the first shell by three oxygen atoms in a trigonal-pyramidal sphere with As–O distances at 1.785(±0.03) Å (*20*). In comparison with the curve fit results (Table 2), the reliability of this analysis technique

TABLE 2

Results of Curve Fit Analyses for As–O Shells

	r_j[Å]	N_j	σ^2 (Å^2)
As_2O_3	1.77	2.93	0.00117
H500p4400h	1.67(±0.02)	3.3(±0.3)	0.0001
	1.94(±0.06)	0.7(±0.5)	0.0167

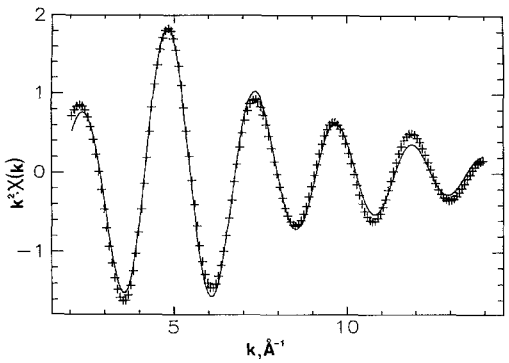

FIG. 5. Curve fit of the Fourier-filtered EXAFS (As–O shells) in H500p4400h (+ experimental; —fit).

according to the concept of chemical transferability is adequate. Hence, in H500p4400h the first oxygen shell around the As^{5+} atoms contains three oxygen atoms at an average radial distance of 1.67 Å. The second shell bears only one oxygen atom with an As–O distance of around 1.94 Å and a high Debye–Waller factor. This (3 + 1) oxygen coordination around As^{5+} and its distance distribution is typical for isolated orthoarsenates(V), $AsO_3(OH)^{2-}$, which are present in the structure of $Na_2HAsO_4 \cdot 7H_2O$ (*21*, *22*).

DRIFT Spectra of Poisoned Catalysts

Information on the interaction of this orthoarsenate(V)-like phase with the catalyst surface can be obtained by vibrational spectroscopy. The *in situ* DRIFT spectra of the samples TiW3A and TiW9A and those of the same samples after deposition of arsenious oxide, TiW3A(As) and TiW9A(As), are shown in Figs. 6a and 6b. Prior to poisoning, TiW3A and TiW9A give rise to bands in the hydroxyl stretching region at 3600–3750 cm^{-1}. These bands are due to titania hydroxyl groups remaining after the anchoring of the tungsten oxide (Fig. 6a). These bonds are relatively broad compared to those observed on pure titania. This is presumably due to perturbation of TiOH groups by the surface tungstate. The bands might also contain contributions from WOH groups. Also the overtones of the W=O modes of the isolated and exposed tungsten oxogroups in the supported phase are observed at 2005 cm^{-1} (Fig. 6b), the intensities of which are proportional to the loading by tungsten oxide on titania (*5*). On sublimation of arsenious oxide onto the surface of samples TiW3A and TiW9A, the titania hydroxyl groups are completely replaced by a new, sharp absorption band at 3610 cm^{-1} on samples TiW3A(As) and TiW9A(As) (Fig. 6a). Similarly, the deposition of As_2O_3 on the surface of pure titania led to the formation of an analogous band at 3620 cm^{-1} with simultaneous erosion of the characteristic hydroxyl bands of titania (*19a*). An equivalent band can also be detected on the surface of As_2O_5 but not on that of As_2O_3 (*23*). We attribute this new absorption band to an As^{5+}–OH group of the proposed orthoarsenate(V) with the estimated As–O distance of 1.94 Å. The W=O overtones are also perturbed by the formation of the orthoarsenate(V) (Fig. 6b). An analogous perturbation of overtones of the tungsten oxogroups occurs by the adsorption of Lewis bases such as H_2O, NH_3, or CO on the coordinatively unsaturated tungsten sites of the supported tungsten oxide (*5*). This indicates

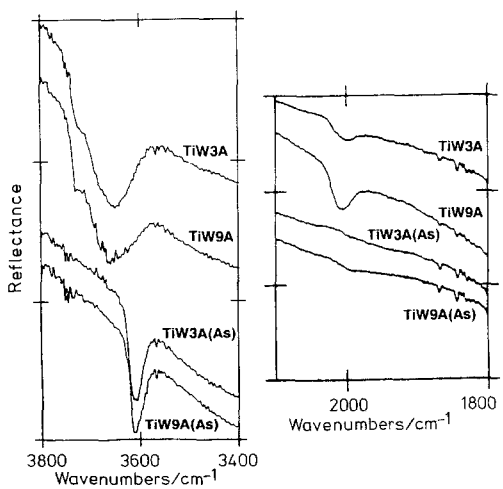

FIG. 6. *In situ* DRIFT spectra of TiW3A (1), TiW9A (2), TiW3A(As) (3), and TiW9A(As) (4) at 673 K in O_2.

that probably the same chemisorption centers are involved. The same changes by the orthoarsenate(V) adlayer are also observed in the DRIFT spectra of the MoO_3/TiO_2 samples, with a Mo=O overtone band at 1968 cm^{-1}.

XANES at W L_1 and W L_3 Edges

We have reported (*24*) W L_1 and W L_3 XANES spectra of identical samples TiW3A and TiW9A, measured at 300 K in air and *in situ* at 673 K in O_2. The position and intensity of the pre-edge peak in the W L_1 edge and the shape and full width at half maximum (fwhm) of the "white line" in the W L_3 edge showed a characteristic behavior for these samples. At 300 K in air the XANES features of TiW3A and TiW9A were very similar to those of $WO_3 \cdot H_2O$. However, after the removal of coordinated water *in situ* at 673 K in flowing O_2, the intensity of the pre-edge peak in the W L_1 edge of TiW3A ($\frac{1}{3}$ monolayer tungsten oxide) increased significantly and the energy position of this *s-d* transition was lowered by 2.1 eV (Fig. 7a). The white line in the W L_3 edge of TiW3A became narrower. The fwhm was then 5.8 eV as compared with 8.0 eV for WO_3 or $WO_3 \cdot H_2O$ and 5.3 eV for Na_2WO_4.

For the sample TiW9A with approximately a monolayer of tungsten oxide, the position of the pre-edge peak in the W L_1 edge shifted by 1.2 eV to lower energy and its intensity increased slightly (Fig. 8a). At 673 K in O_2 the resonance line in the W L_3 edge of TiW9A was 7.1 eV wide. According to the "fingerprint" procedure with XANES spectra of tungsten oxide standard compounds, these observations were interpreted as follows (*24*): tungsten sites on the titania-supported phase are pseudo-octahedrally surrounded by oxygen atoms in ambient atmosphere, comparable to tungsten in $WO_3 \cdot H_2O$. This coordination is independent of the WO_3 loading. At 673 K in O_2 the coordinated water desorbs and the average oxygen coordination number of the tungsten atoms decreases, the reduction in coordination being more pronounced for sample

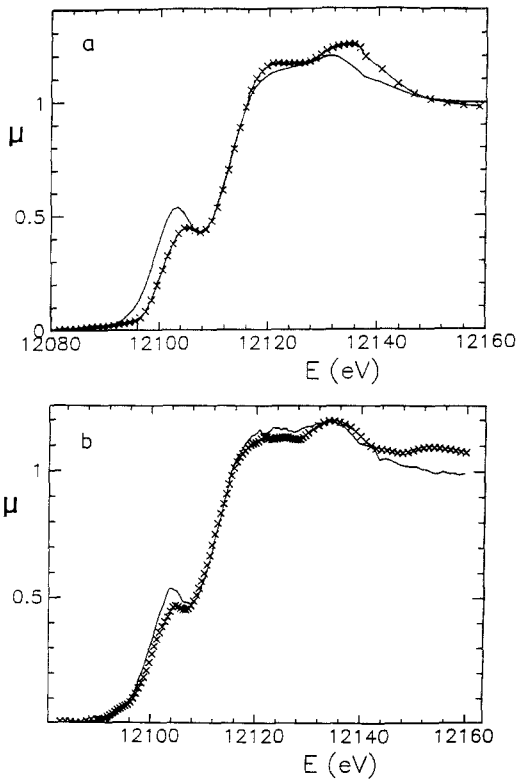

FIG. 7. (a) Normalized W L_1 XANES spectra of TiW3A at 300 K in air (X) and at 673 K in O_2 (—) (from Ref. (24)). (b) Normalized W L_1 XANES spectra of TiW3A(As) at 77 K in N_2 (X) and at 673 K in O_2 (—).

TiW3A with $\frac{1}{3}$ monolayer tungsten oxide than for the monolayer sample TiW9A.

We concluded (*24*) that the tungsten oxide is built up by tetrahedral WO_4 and pentahedral WO_5 units with tungsten in the +6 oxidation state. At a low WO_3 loading of the order of $\frac{1}{3}$ monolayer the WO_4 units predominate, whereas at a monolayer the WO_5 units seem to be more abundant. For the arsenious oxide-poisoned samples TiW3A(As) and TiW9A(As) the W L_1 XANES features at 77 K in N_2 (Figs. 7b and 8b) compare extremely well in energy position and intensity of the pre-edge peak with those of the unpoisoned samples TiW3A and TiW9A at 300 K in air. Since the edge positions remain unchanged, the tungsten atoms are still hexavalent despite the presence of the proposed orthoarsenate. On heating to 673 K in O_2 the

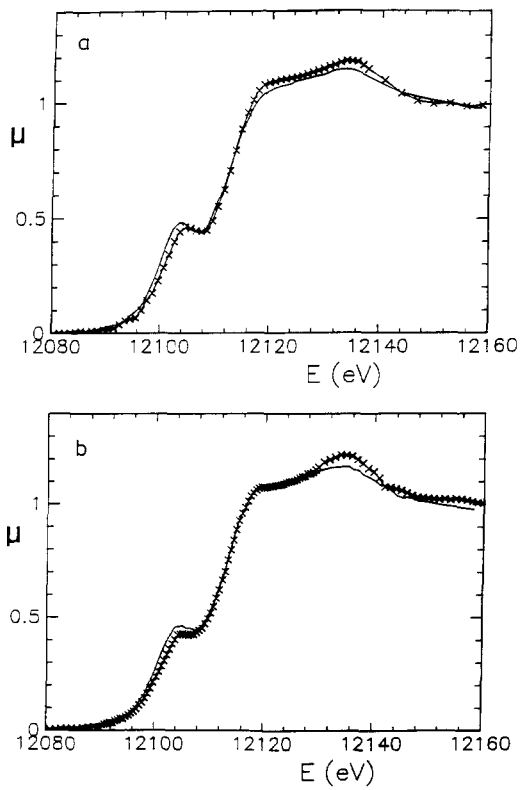

FIG. 8. (a) Normalized W L_1 XANES spectra of TiW9A at 300 K in air (X) and at 673 K in O_2 (—) (from Ref. (*24*)). (b) Normalized W L_1 XANES spectra of TiW9A(As) at 77 K in N_2 (X) and at 673 K in O_2 (—).

intensity of the pre-edge peak in the W L_1 edge of TiW3A(As) (Fig. 7b) and of TiW9A(As) (Fig. 8b) increase also in the same order as observed for the samples TiW3A and TiW9A, respectively (*24*). The low-energy shift of the pre-edge peak in the W L_1 edge is -0.9 eV for TiW3A(As) and -0.1 eV for TiW9A(As). These values are significantly smaller than the shifts observed earlier for TiW3A (-2.1 eV) and TiW9A (-1.2 eV) (*24*). The fwhm of the W L_3 white line in TiW3A(As) and in TiW9A(As) is 7.4 eV at 673 K in O_2, compared with 5.8 eV for TiW3A and 7.1 eV for TiW9A.

Based on the W L_1 and W L_3 XANES fingerprint spectra of a variety of reference compounds, as discussed in Ref. (*24*), the present results suggest that the average oxygen coordination number of the tungsten sites is increased on poisoning of WO_3/TiO_2 catalysts by deposition of arsenious oxide relative to the dehydrated state of the catalyst. These XANES results indicate that an interaction of the orthoarsenate with the surface tungsten sites occurs, consistent with the DRIFT investigations as mentioned above. Unfortunately, for sample TiW3A(As), substantial amounts of As^{3+}, probably in the form of amorphous As_2O_3, are present besides the orthoarsenate, and the nature of interaction of these two arsenic species with the tungsten coordination sphere cannot be separated. However, for sample TiW9A(As) the arsenic is almost exclusively present as orthoarsenate, and the differences in the W L_1 pre-edge energy and W L_3 white line fwhm between 77 and 673 K are negligible. Thus, even at 673 K the tungsten sites of the monolayer tungsten oxide are pseudo-octahedrally surrounded by oxygen. Since for orthoarsenate(V) Lewis-basic properties, as, e.g., for NH_3, are not to be expected, the only possible mode of interaction of an orthoarsenate is a chemical W–O–As bonding.

At this stage of the investigation, the assignment of the described interaction to a chemical W–O–As bonding is tentative, because the presently available EXAFS analysis does not give any evidence of either As–As or of As–W distances. A particular difficulty is the fact that at present only one structurally defined W/O/As compound which could be used as a reference is known, namely $W_2O_3(AsO_4)_2$ (*25*). Further investigations are needed to obtain direct evidence of a W–O–As bonding, although there is no doubt that the orthoarsenate(V) interacts strongly with tungsten sites.

Admittedly, the surface arsenate species can also be formed on islands of uncovered titania support surface, the relative amounts at saturation depending on the tungsten oxide loading.

CONCLUSION

The present XAS and DRIFT results demonstrate for the first time that the As_4O_6

molecules in the As_2O_3 gas phase are catalytically oxidized to a surface orthoarsenate(V) by Ti/W, Ti/Mo, and Ti/Mo/V catalysts, and also by pure TiO_2. This result is independent of the process of poisoning by arsenious oxide. Only at low coverage of active components (WO_x, MoO_x) on titania or for the free titania surface are considerable amounts of As^{3+} still present, probably as amorphous As_2O_3. Part of the surface orthoarsenate(V) is anchored on the titania surface via titania hydroxyl groups located on patches of the support surface which remained uncovered by the active phase. This species bears itself a hydroxyl group. The remainder of the orthoarsenate(V) interacts with the supported molybdenum and tungsten oxide, which is documented by the strong perturbation of the M=O (M = W,Mo) overtones. XANES investigations at the W L_1 and W L_3 edges confirm the chemical interaction of the tungsten centers with orthoarsenate(V). The local environment around the tungsten absorber is modified, leading to an increased coordination number by oxygen atoms as compared with the dehydrated state of the catalyst. The oxidation state of the tungsten centers remain unchanged as W^{6+}, and there is evidence for the formation of W–O–As bonds. For WO_3/TiO_2 catalysts a correlation of the $deNO_x$-activity with the total acidity, which is composed of the enhanced Brønsted-acidity of the unreacted TiOH groups and of the Lewis-acidity of the coordinatively unsaturated tungsten sites, was found (*5*).

Hence, the formation of the orthoarsenate with W–O–As anchoring bonds and the resulting blocking of coordinatively unsaturated tungsten sites may be considered as being responsible for the deactivation of $deNO_x$-catalysts by arsenious oxide. In addition, a physical obstruction of the pore system of the catalyst framework may also occur.

ACKNOWLEDGMENTS

We thank Siemens AG, München for financial support, and the HASYLAB (DESY Hamburg) for experimental assistance.

REFERENCES

1. Bosch, H., and Janssen, F., *Catal. Today* **2,** 369 (1988).
2. (a) Vogel, D., Dissertation, Universität Erlangen-Nürnberg, Germany, 1989. (b) Balling, L., and Hein, D., "Katalyse," DECHEMA Monogr., Vol. 118, p. 55. VCh-Verlagsgesellschaft, Weinheim, 1989.
3. Gutberlet, H., *VGB Kraftwerkstech.* **68,** 287 (1988).
4. Leyrer, J., Margraf, R., Taglauer, E., and Knözinger, H., *Surf. Sci.* **201,** 603 (1988).
5. Hilbrig, F., Göbel, H. E., Schmelz, H., and Knözinger, H., in preparation.
6. van Hengstum, A. J., Thesis, Twente University of Technology, Enschede, The Netherlands, 1984.
7. Bond, G. C., Flamerz, S., and van Wijk, L., *Catal. Today* **1,** 229 (1987).
8. Lytle, F. W., Sayers, D. E., and Stern, E. A., *Phys. Rev. B* **11,** 4825 (1975).
9. Lengeler, B., and Eisenberger, P., *Phys. Rev. B* **21,** 4507 (1980).
10. Lee, P. A., Citrin, P. H., Eisenberger, P., and Kincaid, B. M., *Rev. Mod. Phys.* **53,** 769 (1981).
11. Bart, J. C., *in* "Advances in Catalysis" (D. D. Eley, H. Pines, and P. B. Weisz, Eds.), Vol. 34, p. 203. Academic Press, San Diego, 1986.
12. Koningsberger, D. C., and Prins, R., Eds., "X-Ray Absorption: Principles and Techniques of EXAFS, SEXAFS and XANES." Wiley, New York, 1989.
13. Lengeler, B., *Microchim. Acta (Wien)* **1,** 455 (1987).
14. (a) Lengeler, B., *Festkörperprobleme* **29,** 53 (1989); (b) Lengeler, B., *Adv. Mater.* **2,** 123 (1990); (c) Lengeler, B., *Phys. Bl.* **46,** 50 (1990).
15. *Struct. Rep.* **11,** 380 (1947/1948).
16. Jansen, M., *Z. Anorg. Allg. Chem.* **441,** 5 (1978).
17. Agarwal, B. K., and Verma, L. P., *J. Phys. C* **1,** 208 (1968).
18. Sapre, V. P., and Mande, C., *J. Phys. C* **5,** 793 (1972).
19. (a) Lange, F., Schmelz, H., and Knözinger, H., submitted; (b) Rademacher, I., Borgmann, D., and Wedler, G., personal communication.
20. Bötticher, H., Plieth, K., Reuber-Kürbs, E., and Stranski, I. N., *Z. Anorg. Allg. Chem.* **226,** 302 (1951).
21. Ferraris, G., and Chiari, G., *Acta Crystallogr., Sect. B* **26,** 1574 (1970).
22. Baur, W. H., and Khan, A. A., *Acta Crystallogr., Sect. B* **26,** 1584 (1970).
23. Ramstetter, A., unpublished results.
24. Hilbrig, F., Göbel, H. E., Schmelz, H., and Lengeler, B., submitted for publication.
25. Westerlund-Sundbäck, M., *Acta Chem. Scand.* **25,** 1429 (1971).